



Characterizing Khetri copper mine environment using geospatial tools

Anita Punia^{1,2}  · Pawan Kumar Joshi^{1,3} · Neelam Siva Siddaiah¹

Received: 13 August 2020 / Accepted: 7 January 2021 / Published online: 22 January 2021

© The Author(s) 2021 

Abstract

Mines result in land use and land cover (LULC) change due to degradation of natural resources and establishment of new infrastructure for ore extraction and beneficiation. The present study was carried out to, with objectives, (1) characterize LULC change (from 1975 to 2017) in Khetri copper mine region, (2) spatial distribution of pollution indices and (3) spectral response of elemental concentration of soil and groundwater using Landstat and ASTER satellite data. The study was designed to fulfil the objectives and for the same NDVI values were calculated for LULC classification and generated maps were analyzed for landscape pattern. Spatial distribution of pollution indices calculated using geochemical data of soil and groundwater was plotted to understand the impact of contamination on landscape pattern. The correlation of spectral response of Landstat bands with heavy metals concentration was plotted to assess their possible use in quantification of heavy metals. Results show constant increase in settlements, mines and open area while vegetation cover has decreased. Landscape and class level metrics (number of patch, patch density, aggregation index and landscape shape index) indicate increase in the fragmentation of landscape in recent years. Shannon's Evenness Index indicates increase in uniformity in landscape and it is attributed to loss of vegetation and agriculture patches. Pollution indices, Pollution Load Index for soil is high near the overburden materials and Index of Environmental Risk (I_{ER}) and Contamination Index for ground water is high near abandoned mines. Spectral bands 5 and 6 (SWIR 1) show significant negative correlation, and 9 (Cirrus) shows significant positive correlation with metal concentration in soil and water suggesting the possible use of remote sensing in assessment of metal concentration at ground level. Thus, it can be concluded that mines significantly influence the landscape pattern and remote sensing could be used for the assessment and predication of heavy metal contamination at broader scale in a cost-effective way.

Keywords Underground mine · Pollution · LULC · Landscape metrics · Spectral reflectance

1 Introduction

Mines are important for any economy but have significant adverse impact on environment [1]. Extensive mining leads to changes in land use and land cover (LULC) [2, 3]. Pollutants and waste generated from the mines are one of the major causes for deterioration of soil and water quality [4] which disturbs the ecosystems [5] and thus landscape. The illegal mines also put pressure on the environment and results in degradation of forest cover [6]. Mines lead

to changes in landscape through land transformation, habitat loss and fragmentation. In opencast mining deforestation, urbanization and mine expansion lead to LULC changes [7]. Impact of underground mines on landscape is slow but has significant influence on vegetation [8, 9]. The land subsidence due to underground mines leads to adverse ecological impacts specifically on agriculture [10].

Excavation of ore generates huge quantities of heavy-metal-enriched mining waste. Mining with 1 wt% of ore result in 99% of the total quantity of excavated ore into

✉ Anita Punia, puniaanita12@gmail.com; ✉ Pawan Kumar Joshi, pkjoshi27@hotmail.com | ¹School of Environmental Sciences, Jawaharlal Nehru University, New Delhi 110 067, India. ²Department of Civil Engineering, Indian Institute of Technology, Guwahati, Assam 781039, India. ³Special Centre for Disaster Research, Jawaharlal Nehru University, New Delhi 110 067, India.



waste. Huge piles of mining waste on exposure to oxygen and water generate acid mine drainage (AMD) which decreases pH and facilitates the leaching of heavy metals. High concentration of heavy metals under low pH conditions leads to the contamination of surroundings and poses health risk to human [11]. The extent and intensity of heavy metal contamination due to mining waste is significant in nature. Excessive presence of heavy metals (threshold values for Cu = 19.96, Zn = 49.04, As = 14.05, Sn = 0.19 and Cr = 89.80 mg/kg) in soil inhibits the growth of plants [12]. However, the ecological disturbances caused by open pit mine and waste dumps are different from each other. It is observed that ecology surrounding the open pit mine landscape is severely impacted compared to dumping landscape which has moderate disturbances [13]. Open pit mines cause serious adverse impact on the environment [14] and change in LULC is due to decrease in vegetation cover caused by mining activities [15].

The changes in landscape patterns for more than a century could be divided into major five processes namely urbanization, intensification of agriculture, abandonment, deforestation, and afforestation in the mining region [3]. The displacement of population for mines or abandonment of mines after the extensive ore extraction is also reflected in landscape patterns. The future projection of LULC patterns on the basis of current LULC classification is also feasible to predict. The future projection of landscape pattern would be helpful in managing the land resources in sustainable manner for ecological restoration and protection [16, 17]. Apart from LULC, calculation of vegetation fractional coverage (VFC) and vegetation index (VI) using remote sensing images is found effective in assessing the mining impact on soil and vegetation cover [18].

Construction of ore beneficiation units along with roads on forest land results in deforestation and are potential changes observed on the mining landscape. Establishment of tailing dams, waste rocks dumps, effluent treatment plants, water storage ponds and built-up are the visible changes in landscape pattern caused by the mines [19, 20]. Spatiotemporal characterization of mining landscape indicates the presence of open pits and waste dumps in place of vegetation cover [21, 22]. In the current scenario of urbanization and industrialization, the environmental protection is major concern for society. It is important to understand the LULC changes in mining region for conservation of natural resources and environmental protection.

Tropical and developing countries often report changes in landscape pattern and processes due to human interventions [2, 23, 24]. Changes in diverse landscape are easily visible [25, 26], and their impacts are easily detected [27]. However, in the semi-arid regions, as the landscape looks homogenous with less diversity, the magnitudes of impact are not visible [28, 29]. Thus, often

it is difficult to assess the reason for landscape fragmentation in semi-arid regions which are covered with low vegetation cover. The assessment of LULC changes in semi-arid region due to underground mines needs further research for better understanding the impacts of mines landscape pattern.

The impacts of open pit and underground mines on landscape pattern would be different in nature. Operation of open pit mine in the forest land result in deforestation and the impacts are direct in nature. However, in case of underground mines most of the loss of vegetation cover is due to degradation of soil and water resources or subsidence of land. Dumping of mining waste and establishment of ore processing plant in forest land would results in deforestation in case of underground mines. Thus, the impacts of underground mines on the vegetation cover are visible in long term [9].

Mining for petroleum products, stones and minerals is one of the known commercial activities in the semi-arid region of India [30–32]. But the impact of these on the landscape patterns and soil and water contamination is the least studied [33]. Heavy metal contamination of soil and water due to mining is well reported by many researchers from different parts of the world [34, 35]. Monitoring and assessment of environmental contaminants require extensive laboratory work and time. The aerial extent of large-scale mines is more compared to small-scale mines; hence LULC changes due to large-scale mines are easily detected with satellite imagery than small-scale mines. For the assessment of LULC due to small-scale mine, a high-resolution satellite imagery data is required. It is observed that a high degree of accuracy could be achieved for the assessment of LULC change caused by small scale and illegal mines through the application of deep convolutional neural network model using Sentinel-2 multispectral satellite imagery [36].

Bands of satellite imagery are used to develop the models for the predication of values of water quality parameter. The models developed using the bands of Landsat 8 and Sentinel-2 data are found more suitable for the surface water quality assessment compared to ASTER and SPOT 6 [37]. Satellite imagery with higher number of bands is more suitable for the models. Optically active water quality parameters such as turbidity, blue–green algae phyco-cyanin and chlorophyll-a content could be assessed with high accuracy using the satellite imagery for fast and easy assessment [38]. Statistical relation between the ASTER bands and water quality parameters (temperature, pH, total dissolved solids, salinity, total alkalinity, electrical conductivity, ortho-phosphorus and total organic carbon) is found suitable for their accurate predication and generation of spatial distribution maps through regression analysis [39].

Heavy metals are minor constituents of soil, so their detection using spectral signatures is a difficult task. Heavy metal concentration should exceed 4 ppm to be detected from spectral signature [40]. Heavy metals show strong correlation with organic matter, and their relation can be used for remote prediction and estimation of heavy metals [41, 42]. But the concept is not applicable to sites having low content of organic matter like arid or mining areas. Correlation between the pixel values of satellites imagery and analyzed parameters in soil and water is continuously being monitored for the development of suitable prediction model. Nadari et al. [43] reported that the assessment and prediction of heavy metals around the contaminated sites using stepwise multiple linear regression and neural network-genetic algorithm model based on visible/near-infrared reflectance of electromagnetic range of satellite imagery provides reliable information. Thus, relation between satellite spectral response and elemental concentration in soil is needed to be study.

Heavy metals also show strong correlation among themselves and the phenomena could be used for the assessment of heavy metals [44, 45]. The heavy metals also have strong correlation among themselves, i.e., two heavy metals might be found in association with natural conditions. But correlation among heavy metals is site specific and depends upon their source. Thus, the applicability of this phenomena at a global level is debatable. Sensitivity of spectral bands is metal specific and waveband selection is important criteria for assessment of metal content in soil. Studies have suggested different wavebands for different metals such as wavebands centered about 460, 1400, 1900 and 2200 nm are more sensitive for As and Cu [45] and bands centered around 838, 1930 and 2148 nm are sensitive for Pb content.

Application of LULC in assessment of environmental impacts of mines is fast and economical compared to other impact assessment methods [46]. It also generates maps indicating the mining impacts on environment which is a cost-effective method compared to field-based monitoring. The classified LULC maps could be used to understand the change in landscape pattern. Heavy metal contamination of soil and water is commonly found in the mining region so the spatial distribution of heavy metals using the geospatial tools has been proposed to done to understand the impact of contamination on landscape pattern. Field-based estimation of heavy metals is a lengthy process; hence, correlation of geochemical data with spectral reflectance of Landsat data for fast identification is proposed. The relation would open door for further research in inventing the estimation method for heavy metal using the spatial tools. With this background, the present study was designed to characterize Khetri copper mine environment. The objectives of the study are to (i) assess the

changes in LULC between 1975 and 2017, (ii) assess the impacts of mines using landscape metrics and pollution indices and (iii) to estimate relationship between satellite spectral response and elemental concentration in soil and groundwater.

2 Study area

Khetri copper complex (KCC) mines are located in north-western part of India and are active since 1973 (Fig. 1). These are located at an altitude of 550 m above mean sea level with geographic location, 28°04'21.17" north latitude and 75°49'23.29" east longitude. The area falls in sub-tropical, semi-arid region with mean annual rainfall around 500 mm. The region is covered with sparse vegetation, and the major species include *Prosopis cineraria*, *Ziziphus jujube*, *Prosopis juliflora*, *Azadirachta indica* and *Vachellia karro*. Agricultural is practiced in two major seasons Kharif (July–October) and Rabi (October–March).

The KCC belt extends about 80 km in length from Singhana (Jhunjhunu district) in the northeast to Sangarva (Sikar district) in the southwest. The KCC mines are active at Khetri and Kolihan and not at Chaandmari, which is abandoned since 2002. All mines at KCC are underground except Chaandmari, which cover small area. The mine generates huge quantity of sulfide rich waste such as tailings and overburden materials. For the last few decades, a huge quantity of waste is being dumped openly in the environment of Khetri covering a large area. In the region, dust storms blow from south-western direction during summer (May–June) and from northwestern direction during winter (December–January). The tailings by virtue of their fine-grained nature are easily carried away to distant places by these winds. In addition, metals can easily be leached from these dumps and contaminate the surface and groundwater.

3 Materials and methods

To assess changes in LULC after the implementation of mines in semi-arid region, satellite images of 1975 (Landsat-MSS) and 2002, 2012 and 2017 (Terra-ASTER) were downloaded from the United States Geological Survey (USGS) earth explorer website (<https://earthexplorer.usgs.gov/>). The vegetation cover depends upon the intensity and duration of rainfall so images of monsoon season were avoided. The satellite images of pre-monsoon season (March) were selected for classification. Details of the satellite images used are given in Table 1.

For image pre-processing and classification, ERDAS 9.1 software was used. Normalized Difference Vegetation

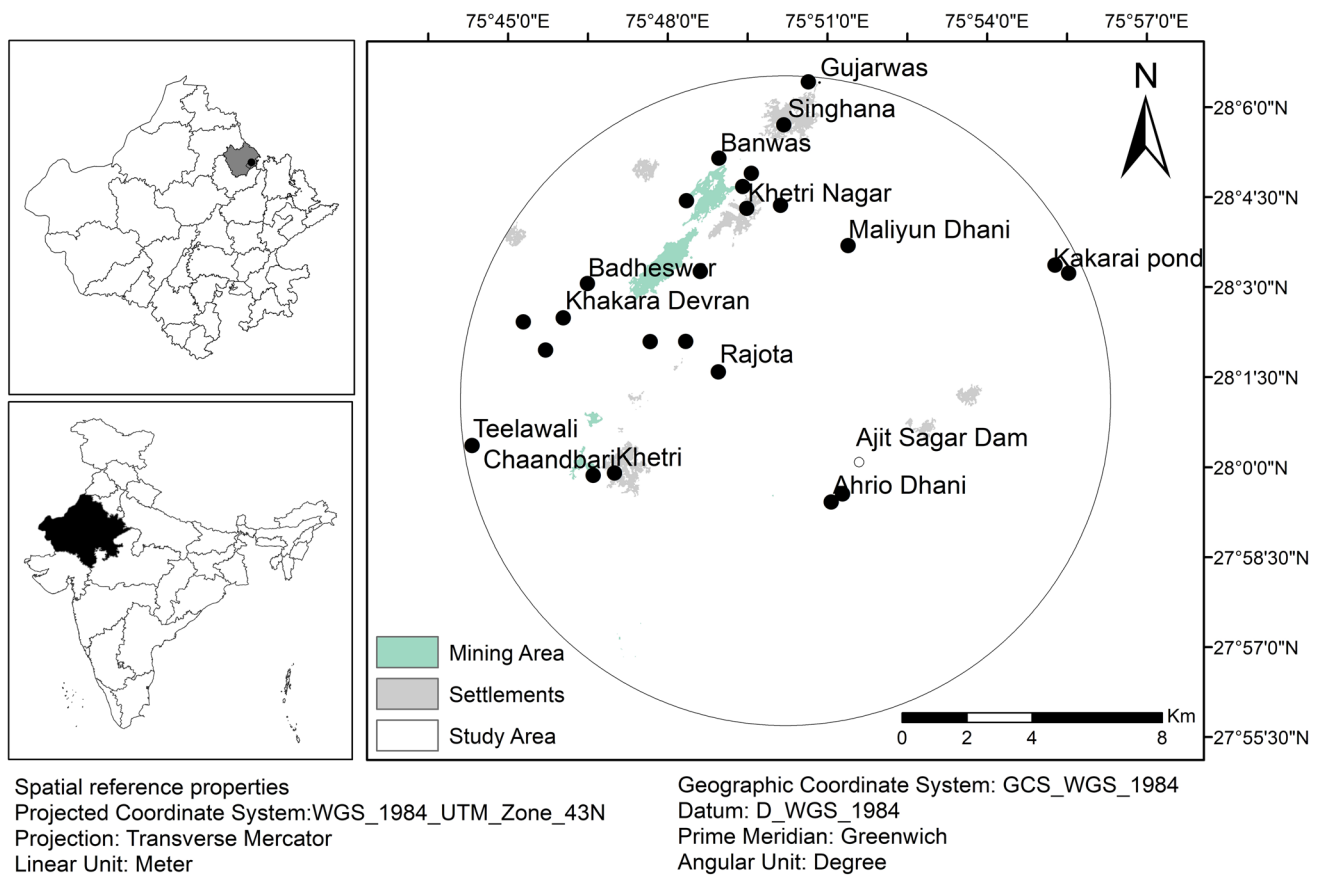


Fig. 1 Map showing location of study area and distribution of mines and settlements

Table 1 Details of satellite images used for LULC mapping

Satellite	Date	Path/Row	Spatial resolution (m)	Swath (km)	Spectral resolution (µm)
Landstat MSS (level 1)	02 March 1975	158/41	80	185	Band 1 (0.5–0.6)
					Band 2 (0.6–0.7)*
					Band 3 (0.7–0.8)*
					Band 4 (0.8–1.1)*
Terra ASTER (level 1 T)	18 March 2002	147/41	15	60	Band 1 (0.52–0.60)*
					Band 2 (0.63–0.69)*
					Band 3 (0.76–0.86)*
					Band 4 (1.60–1.70)
					Band 5 (2.14–2.18)
					Band 6 (2.18–2.22)
					Band 7 (2.23–2.28)
13 March 2012	147/41	15	60	Band 8 (2.29–2.36)	
				Band 9 (2.36–2.43)	
				Band 10 (8.12–8.47)	
				Band 11 (8.47–8.82)	
				Band 12 (8.89–9.27)	
				Band 13 (10.25–10.95)	
				Band 14 (10.95–11.65)	
04 March 2017	147/41	15	60		

*Bands used in the present study

Index (NDVI = $\frac{NIR - R}{NIR + R}$) images created from false color composite (FCC) (bands 432 for LandstatMSS and 321 for ASTER) were used for classification. NDVI image was more useful in differentiating vegetative areas from the non-vegetative areas. The NDVI images were clustered using Iterative Self Organizing Data Analysis (ISODATA) technique (clusters = 100, iteration = 24, and convergence level 0.99). Buffer shape file of radius 10 km was overlaid on the NDVI image covering the mining region and downwind direction of mines. The scarce vegetation with diverse geology could result error in LULC classification; hence, ground truth points were used for the post-classification refinement of the misclassified pixels.

NDVI-based LULC classification is widely used for spatiotemporal differentiation of vegetation cover from other classes [34–37, 47–50]. The calculated values of NDVI range from (–)1 (no vegetation) to (+)1 (vegetation) [51]. Low values of NDVI indicate the bare soil and high values of NDVI indicate the dense vegetation cover. NDVI are used for understanding the changes in vegetation cover depending on the chlorophyll content and other factors related to plant growth [52]. The study area is covered with scattered vegetation and it is difficult the vegetation covers from other classes. Mines are well known for adverse impacts on the vegetation cover [53, 54]; hence, for the classification NDVI values were used.

For LULC, the clusters were classified into seven classes namely mines, settlements, agriculture, current fallow, open area, vegetation and water body. The pixels with highest NDVI values were classified as agriculture. Mining infrastructure, tailings and overburden material are included in mine class. The pixels with medium NDVI were classified as vegetation, and it includes the areas covered with the high density of local and invasive trees. The low NDVI pixels were classified as open area with very low density of vegetation. The accuracy assessment was carried out using random points covering all mapped classes. Overall accuracy and kappa coefficient were computed. The overall accuracy varies from 83% (1975) to 86% (2017) with kappa coefficient from 0.81 to 0.85. The accuracy assessments for 2002 and 2012 are 85 and 84% with kappa coefficients 0.85 and 0.83, respectively, being observed.

The landscape metrics were calculated using Fragstats 4.2.1 software [55] (Table 2). Fragstat is frequently being used to detect landscape fragmentation on the basis of landscape metrics [56, 57]. These are combination and arrangement of patch of different shapes and sizes [58]. Seven pattern indices namely number of patches (NP), edge density (ED), landscape shape index (LSI), patch density (PD), aggregation index (AI), contagion index (CONTAG) and Shannon's evenness index (SHEI) were used at landscape level. Seven pattern indices namely AI, ED, NP, core area (CA), total edge (TE), largest patch index (LPI)

and interspersed juxtaposition index (IJI) were used at class level.

Geochemical data for soil and groundwater calculated by Punia and Siddaiah [59] and Punia et al. [33] were used for representing the spatial distribution of pollution indices. The extent of pollution load in soils is evaluated using Pollution Load Index (PLI) and in groundwater using Contamination Index (CI) and Index of Environmental Risk (I_{ER}). PLI is to assess the number of times by which overall metal concentration exceeds the background concentration in particular sample. CI evaluates the enrichment of metals with respect to maximum permissible limits of BIS (2012). I_{ER} predicts the probability of the occurrence of the negative impact on the environment by means of specific contaminations. Map showing the spatial distribution of pollution indices for soil and groundwater was plotted using ArcMap 10.1 software.

Metal concentration in soil and groundwater in the study area as reported by Punia et al. [33], and Punia and Siddaiah [59] was used. The results of above study were used because concentrations of different metals show spatial variation. The satellite images (Landstat 8, observation dates 15th September and 23rd March, 2015) within the 2–3 days of the sampling date (19–21st March and 17–18th September, 2015) mentioned by above authors were downloaded from the USGS earth explorer website (<https://earthexplorer.usgs.gov/>). The correlation between the pixel values of different bands of satellite images and the chemical composition of soil and groundwater was calculated to understand the response on the satellite data. Methodology flowchart indicating all the steps process is shown in Fig. 2.

4 Results and discussion

Loss of vegetation cover or agricultural land because of opencast mining is well studied [60]. The impact of underground mine on LULC change is less studied. In the following sections, LULC change due to underground mines in semi-arid region is being discussed.

5 Land use and land cover (LULC) change

The area covered by mines increased from 1.02 to 1.96 sqkm between 1975 and 2002 with a rate of 0.02 sq km per year. The Kolihan and Khetri mines further showed increase in the rate from 0.02 to 0.04 between 2012 and 2017 (Table 3). Both the mines are underground so their expansion is not visible spatially. But increment in the quantity of overburden and tailings are proportional to the expansion of the mines. Thus, increase in the area

Table 2 List of landscape metrics used for the study

Metrics	Description	Formula
Number of patches (NP) ^{a,b}	Total number of patches in landscape or class	$NP = n_i$ $n_i = \text{number of patches of patch type } i$
Edge density (ED) ^{a,b}	ED is the ratio of edge to area	$ED = \frac{\sum_{k=1}^{mn} e_{ik}}{\sqrt{A}}$ $e_{ik} = \text{total length (m) of edge in landscape involving patch type (class) } i$ $A = \text{total landscape area (m}^2\text{)}$
Landscape shape index (LSI) ^b	LSI is the total length of edge of class	$LSI = \frac{0.25 \sum_{k=1}^m e_{ik}}{\sqrt{\frac{A}{m}}}$ $LSI = \frac{0.25 \sum_{k=1}^m e_{ik*}}{\sqrt{A}}$ $e_{ik*} = \text{Total length (m) of edge in landscape between patch types * (classes) } i \text{ and } k$ $A = \text{total landscape area (m}^2\text{)}$
Patch density (PD) ^b	Number of patches per 100 hectares	$PD = \frac{n_i}{A} (10,000)(100)$ $n_i = \text{number of patches in the landscape of patch type (class) } i$ $A = \text{total landscape area (m}^2\text{)}$
Aggregation index (AI) ^{a,b}	AI shows the aggregation or clumping of patches into a single compact patch	$AI = \left[\sum_{i=1}^m \left(\frac{g_{ii}}{\max \rightarrow g_i} \right) P_i \right] (100)$ $g_{ii} = \text{number of like adjacencies (joins) between pixels of patch type (class) } i$ $\max \rightarrow g_i = \text{maximum number of like adjacencies (joins) between pixels of patch type (class) } i$ $P_i = \text{proportion of landscape comprised of patch type (class) } i$
Contagion index (CONTAG) ^b	Contagion measures the extent to which patch types are aggregated or clumped; higher values indicates large, contiguous patches, whereas lower values generally characterize landscapes with many small and dispersed patches	$CONTAG = 1 + \left[\frac{\sum_{i=1}^m \sum_{m=1}^m \left[P_i \times \frac{g_{ik}}{\sum_{k=1}^m g_{ik}} \right] \times \left[\ln \left(\frac{P_i \times \frac{g_{ik}}{\sum_{k=1}^m g_{ik}}}{\sum_{k=1}^m P_k \times \frac{g_{ik}}{\sum_{k=1}^m g_{ik}}} \right) \right]}{2 \ln m} \right] (100)$ $P_i = \text{proportion of the landscape occupied by patch type (class) } i$ $g_{ik} = \text{number of adjacencies (joins) between pixels of patch types (classes) } i \text{ and } k$ $m = \text{number of patch types (classes) present in the landscape}$
Shannon's evenness index (SHEI) ^b	SHEI is a measure of patch distribution and abundance. High values of SHEI represent more evenness of landscape. It also indicates that mixed class pixels are changed into single class pixels	$SHEI = \frac{-\sum_{i=1}^m (P_i \ln P_i)}{\ln m}$ $P_i = \text{proportion of the landscape occupied by patch type (class) } i$ $m = \text{number of patch types (classes) present in the landscape}$
Core area (CA) ^a	Interior area of patches	$CA = a_{ij} \left(\frac{1}{10,000} \right)$ $a_{ij} = \text{core area (m) of patch } ij \text{ based on specified edge depths (m)}$
Total edge (TE) ^a	Absolute measure of total edge length of a particular patch type	$TE = E$ $E = \text{total length (m) of edge in landscape}$
Largest patch index (LPI) ^a	LPI is a percentage of total landscape area covered by the largest patch and it is measured in percentage	$LPI = \frac{\max(a_{ij})}{A} (100)$ $a_{ij} = \text{area (m}^2\text{) of patch } ij$ $A = \text{total landscape area (m}^2\text{)}$
Interspersion juxtaposition index (IJI) ^a	IJI measures the patch adjacency	$JI = \frac{-\sum_{k=1}^m \left[\left(\frac{e_{ik}}{\sum_{k=1}^m e_{ik}} \right) \ln \left(\frac{e_{ik}}{\sum_{k=1}^m e_{ik}} \right) \right]}{\ln(m-1)} (100)$ $e_{ik} = \text{total length (m) of edge in landscape between patch types (classes) } i \text{ and } k$ $m = \text{number of patch types (classes) present in the landscape}$

^aIs Class level and

^bIs Landscape level metrics

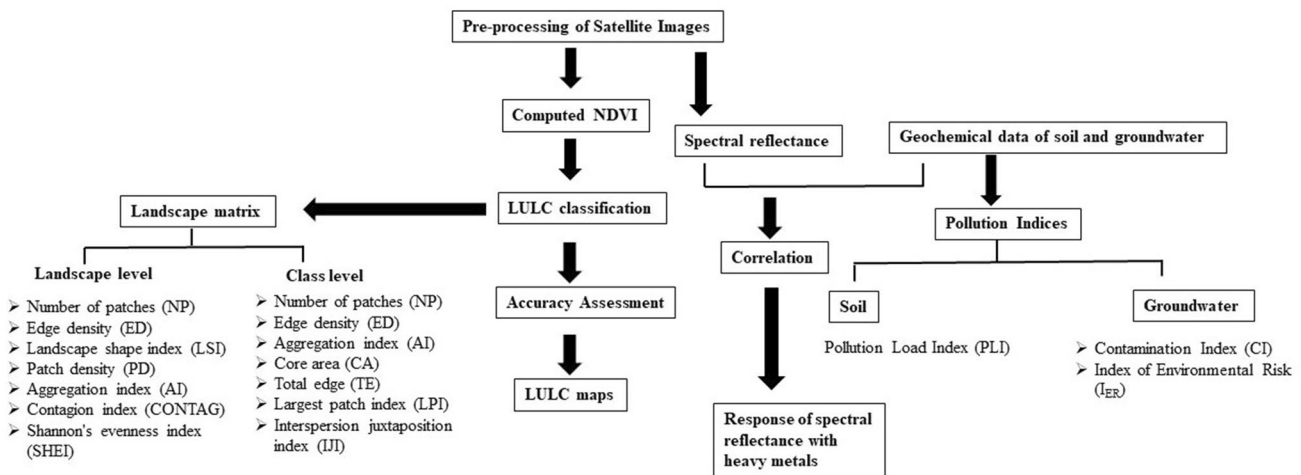


Fig. 2 Methodology flowchart

of underground mines can be attributed to the increase in quantity of waste generated along with the mining infrastructure. Settlements show a consistent increase in the area, i.e., 0.03, 0.07 and 0.09 sq km during 1975–2002, 2002–2012 and 2012–2017, respectively. In the mining region, the construction land increases prominently and impacts the pattern of ecological system [10]. The wells are getting dried off continuously and in some parts groundwater is saline which is not suitable for drinking and agricultural purposes. Despite of drop-off in resources (water and agricultural productivity) in the region, the consistent increase in settlements is indicating expansion of human population. Thus, the population is not migrating despite of degradation of resources.

Earlier studies have reported significant changes in natural landscape due to surface mines [60, 61]. Mines are underground at the KCC; hence, their expansion is not visible on the ground. On comparing the rate of change among settlements and mines, we observed that the rate of change is high for settlements compared to mines (Fig. 3) indicating expansion of human settlements and urban areas in the region. The emergence of mines and related activities enhance the expansion of urban settlements [62]. LULC are important to carry out for environmental protection, as extensive change in LULC could lead to degradation of land and environment [50]. The extraction of ore from the earth already disturbs the upper surface of soil and the impact could be much of greater intensity compared to industrialization and urbanization.

Agricultural land covered 29.56 and 35.87 sqkm of area in 1975 and 2002, respectively. The annual rate of change in agricultural land cover is low (0.01) between 1975 and 2002. While, the annual rate of change of agricultural land cover shows increasing trend (0.03) during 2002–2012.

This is attributed to construction of new wells in this time period, as reported by the locals. During 2012–2017, the agricultural land cover decreased with a rate of 0.20. The increase in salinity along with declining groundwater resources is the reason for decrease in agricultural output. The agricultural fields present in the close proximity of mines are converted to open area between 2012 and 2017. This could be attributed to depletion of groundwater resources or increase in salinity of groundwater.

Vegetation of the region has decreased continuously and its area reduced from 162.23 to 91.71 sqkm since 1975. The undulating terrain of the region is covered with local and invasive trees and is classified as the vegetation class. The declining groundwater level along with increasing mining activities might further accelerate reduction rate of vegetation cover in the semi-arid conditions (high temperature and low precipitation). Decreasing trends of vegetation cover in the study area show similarity with results from other studies carried out by Zhang et al. [18] and Sonter et al. [7]. High concentration of metals could adversely affect the vegetation and other associated processes in the region. The health of plants is adversely affected by high concentration of metals particularly Cu [63, 64]. The decrease in vegetation is observed in the surrounding area of Ajit dam reservoir between 2012 and 2017. The reservoir dried in 2017 and drying of reservoir could be the reason for the decrease in vegetation. While, open area increased continuously from 108 to 164 sqkm from 1975 to 2017. In the semi-arid regions, recovery of vegetation takes the longest time [65].

Mines consume huge quantities of water during ore processing [66], and the world over copper mining alone consumed ~ 1.3 billion cum of water in 2006 [67]. The area covered by surface water bodies decreased with a rate of

Table 3 Area covered by different classes along with their rate of change

LULC classes	1975		2002		2012		2017		Rate of change		
	Area (sqkm)	Area in %	1975–2002	2002–2012	2012–2017						
Mines	1.02	0.34	1.96	0.63	2.85	0.91	3.36	1.07	0.02	0.04	0.03
Settlements	0.87	0.29	2.04	0.65	4.04	1.29	6.29	2.00	0.03	0.07	0.09
Agriculture	29.56	9.75	35.87	11.42	48.43	15.41	17.82	5.68	0.01	0.03	-0.20
Current fallow	0.48	0.16	27.55	8.77	25.03	7.97	30.32	9.66	0.16	-0.01	0.04
Open area	108.73	35.86	122.67	39.05	143.02	45.51	164.29	52.36	0.00	0.02	0.03
Vegetation	162.31	53.54	123.95	39.46	90.86	28.91	91.71	29.23	-0.01	-0.03	0.00
Water bodies	0.21	0.07	0.09	0.03	0.00	0.00	0.00	0.00	-0.03	-0.53	NA

0.05 and 0.02 during 1975–2002 and 2002–2017, respectively, and vanished in 2017. Hence, policies should be implemented for the proper management of groundwater resources. The area lies in semi-arid region, and the degradation of surface water bodies is an alarming situation for the conservation of natural resources. Depletion of water resources directly and indirectly influences the vegetation cover. Interestingly LULC study by Grari and Naryana [68] and Obodai et al. [69] shows the rise in land covered with water due to its release from mines.

LULC are efficient methodology in assessing the land transformation due to mines. In the coal field of Godavari watershed basin, southern India an increase in the infrastructure for mines along with barren land and a decrease in forest cover is observed [68]. The expansion of open cast mines also occupies the surrounding forest or agricultural land [70]. Closed forests change to open forest and further open forests are transformed into the agricultural land, mining area and barren land [69]. LULC also influences the water quality at regional level [71].

6 Landscape and class pattern metrics

Landscapes are geographical areas consisting of interacting ecosystems and human activity [72]. To investigate dynamic changes in landscape patterns, landscape indices such as index of patch, fragmentation index, diversity index, sub-dimension, heterogeneity index and homogeneity index could be used [17]. Application of landscape metrics in understanding landscape pattern of underground mining is hardly an attempt.

Deforestation and mine waste dumps change landscape pattern and fragmentation [17]. The landscape pattern metrics of Muli coal (open cast) mine, China indicate that increase in distance from the mines the fragmentation of landscape decreases [73]. The identification of impact boundary or disturbance ranges using landscape pattern responses is important for the implementation of ecological restoration strategies. Additionally, land subsidence due to underground mines changes and irregularizes landscape patterns, i.e., patch length, shape and size [74].

The landscape pattern metrics were computed at landscape and class levels. SHEI increased from 1975 to 2017 indicating increase in the uniformities of landscape (Fig. 4). Similarly, landscape pattern of Pingshuo opencast coal mine, China a rise in SHEI is observed at landscape level change index suggesting increase in degree of fragmentation due to mines [75]. NP and PD increased from 1975 to 2012 due to increase in fragmentation of landscape while decreased from 2012 to 2017 due to loss of small sized patches. AI decreased from 1975 to 2017 indicating increase in fragmentation. LSI increased from 1975 to 2017

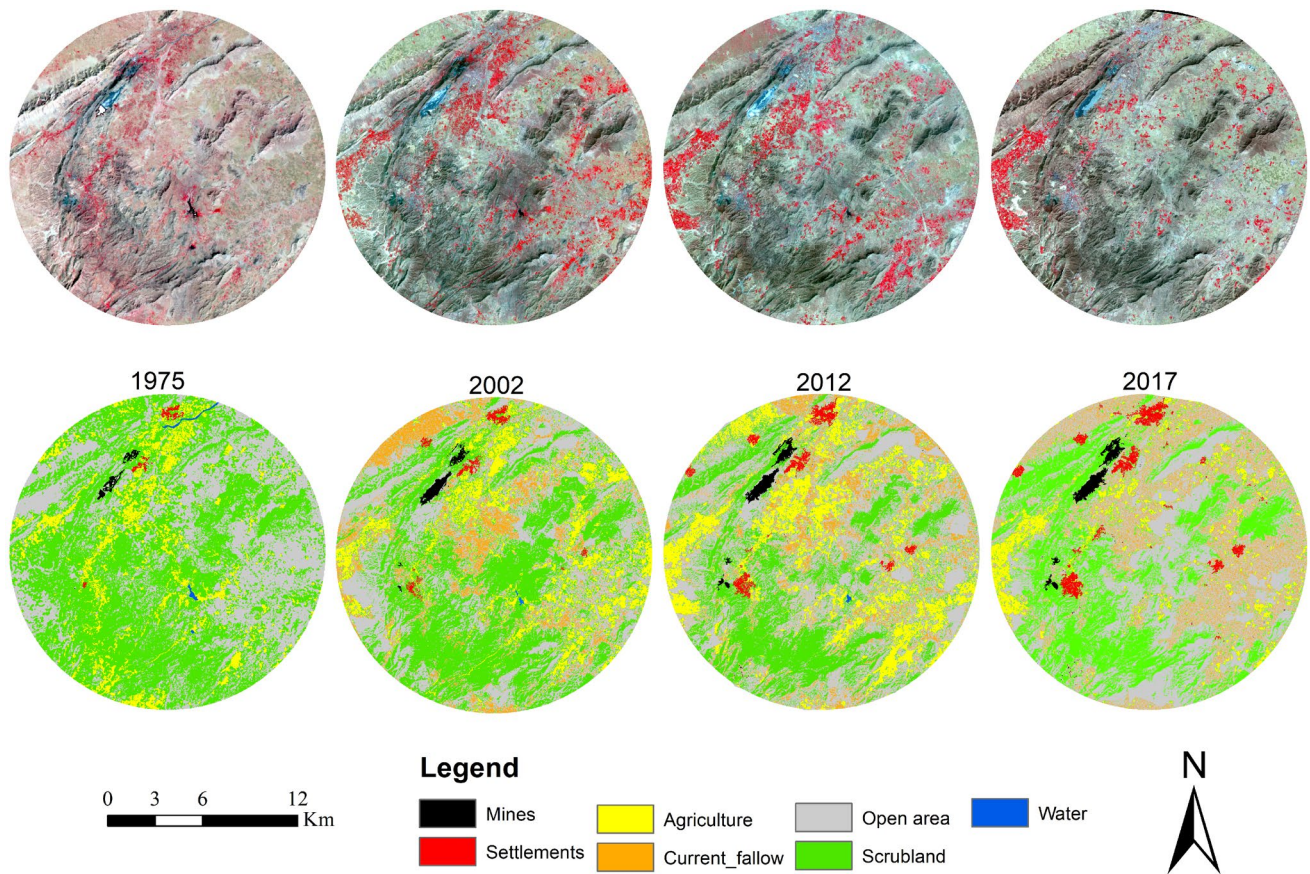
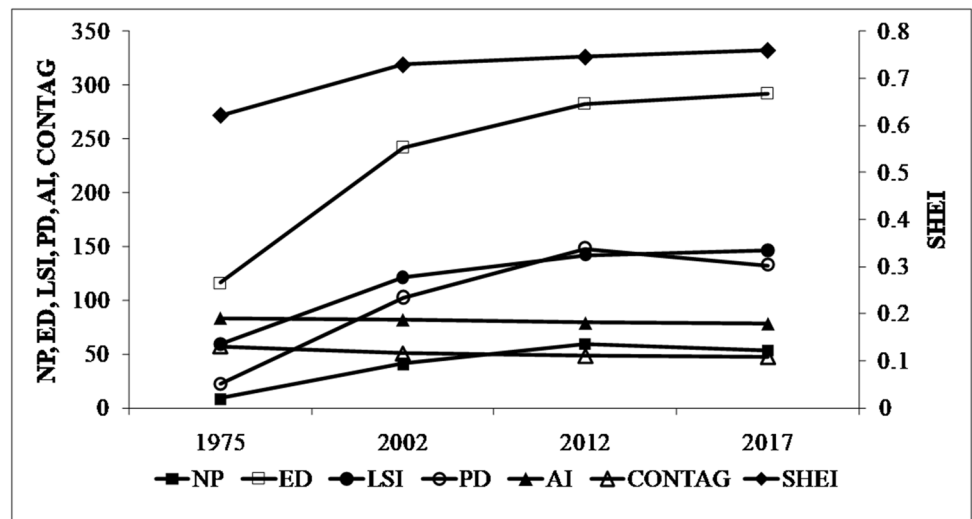


Fig. 3 LULCC maps of Khetri region

Fig. 4 Landscape pattern metrics



indicating fragmentation of landscape. ED increased from 1975 to 2017 indicating decrease in the length of edges compared to area or increase in fragmentation. CONTAG increased from 1975 to 2017 suggesting increase in dispersion or conversion of larger patches to small patches.

Alteration in shape, number and edges of patches have substantial effect on landscape [56].

Both settlements and mines show similarity in distribution pattern of indices at class level. It further confirms that human activities including underground mines strongly

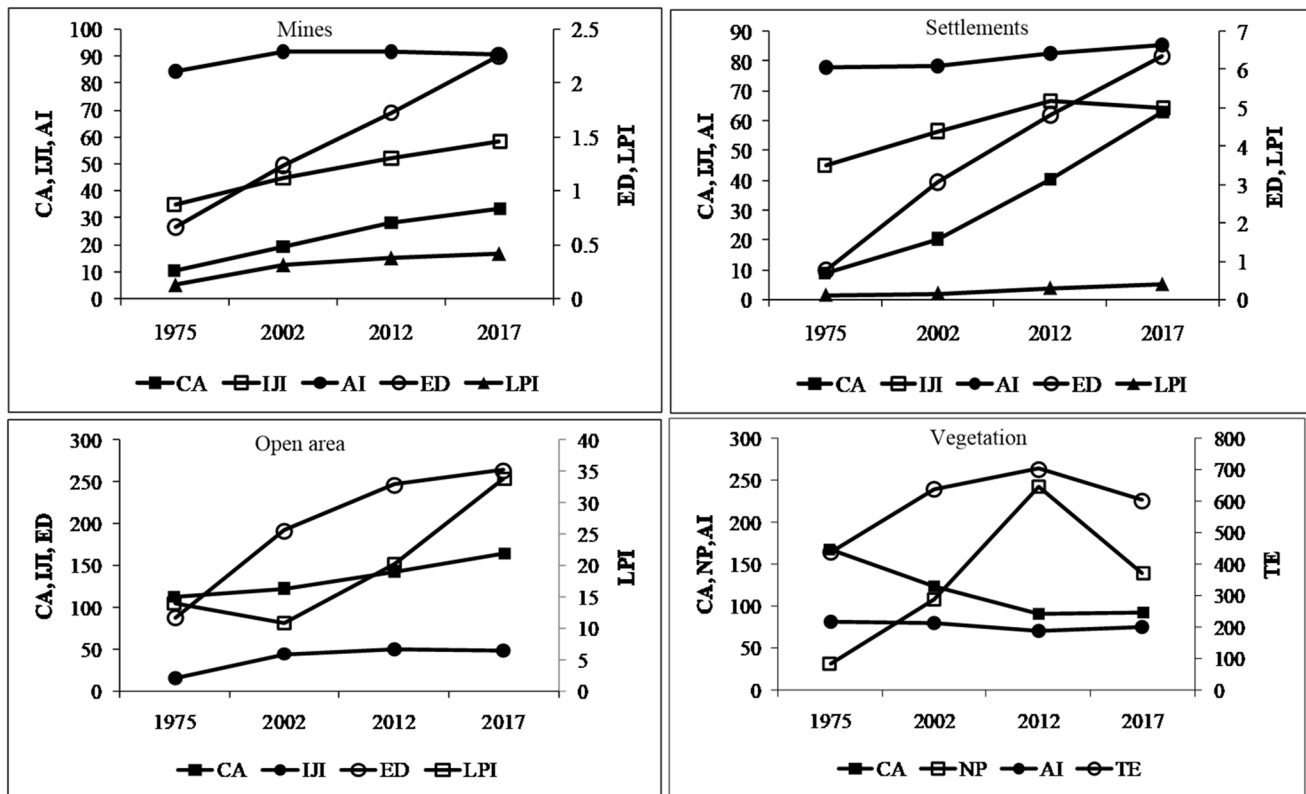


Fig. 5 Class pattern metrics for mines, settlements, open area and vegetation classes

influence local landscape structure resulting in different land uses [76]. CA of mines, settlements and open area increased from 1975 to 2017 indicating increase in area of these classes (Fig. 5). It decreased in case of vegetation, indicating loss or transformation of area covered by vegetation to open area. The ED increased for mines, settlements and open area indicating increase in disturbance or influence of anthropogenic activities. AI and IJI are increasing for both mines and settlements is due to more compaction because of increase in their cover area. LPI increases for mines, settlements and open area suggesting that the area covered by the largest patch area in these categories increases.

Landscape and class level metrics suggest the loss of small patches and increase in the fragmentation. Similar results were observed by some others [2, 77] in the mining landscapes. The mining activities have an adverse impact on the landscape patterns and thus ecosystem.

7 Spatial distribution of pollution indices

The spatial distribution of pollution indices over the study area leads to identify the locations those have high values of pollution indices or most affected locations. Pollution

indices are observed high near the mining sites. Agricultural land those are observed during 1975 and 2002 in the northeast direction of mines are transformed into either current fallow or open area in 2012 and 2017. The over-exploitation of groundwater for mines in addition to high pollution near the mines could be the reason for transformation of agriculture land to current fallow and open area. Extensive pumping of groundwater and LULC change encroach the recharge areas impacting recharge rate of groundwater [78]. High degree of heavy metal contamination has significant influence on the growth of plants because of change in physiological biochemical processes [77]. LULC significantly influences the chemical composition of water resources and alters its quality [71, 79]. The forest area and mine waste contributes significantly to water quality [22] and proper waste management strategies should be adopted.

Pollution index for soil (PLI-soil) is high near the overburden rocks of Khetri mines while the pollution indices for water (CI-water and I_{ER} -water) are high near the abandoned opencast Chaandmari mine (Fig. 6). It suggests that overburden rocks have a high impact on the neighboring soils because fine particles overburden rocks are easily carried away to distant places by strong dusty winds. The abandoned mines have high impact on the groundwater

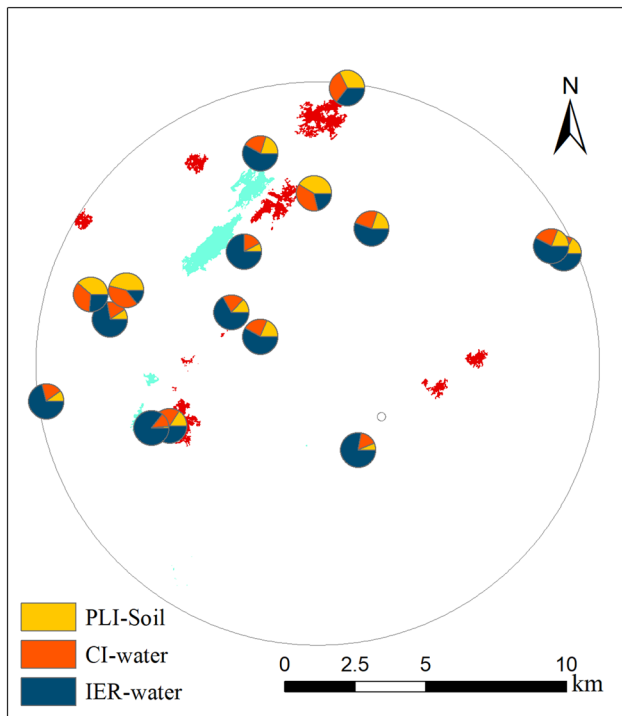


Fig. 6 Spatial distribution of pollution indices

resources as metals get easily leached into the groundwater on exposure to oxygen and water. Mines disturb physico-chemical properties of soil and degrades its quality in terms of nitrogen and organic matter even after the reclamation [80]. Degradation of soil quality is major problem in the restoration of ecology or afforestation due to low fertility [81].

High content of metals in plants can limit their growth [82]. The decrease in the vegetation cover in the windward direction of mines, overburden rocks and tailings is observed. Hence, the present study confirms that the deterioration in quality of soil and water must have resulted in loss of vegetation and decline in agricultural production.

8 Satellite variables vis-à-vis pollution

Study area is enriched with Fe minerals such as pyrite and pyrrhotite [30]. On exposure to oxygen and water Fe-rich minerals generate acid mine drainage (AMD) and secondary minerals. Fe-rich secondary minerals are diagnostic by their spectral signatures [83]. A wide variation in the metal concentration (14–2543 ppm Cu) suggests different chemical composition of soil. Hence, spectral signatures of soil are assumed to vary at different locations. The concentration of Cu can be estimated in soil using spectral reflectance [84]. The application of visible and near-infrared reflectance spectroscopy for the fast

estimation of heavy metals is widely applied [85]; however, the satellite imagery data available based on spectral reflectance for the estimation of heavy metals is neglected in the literature.

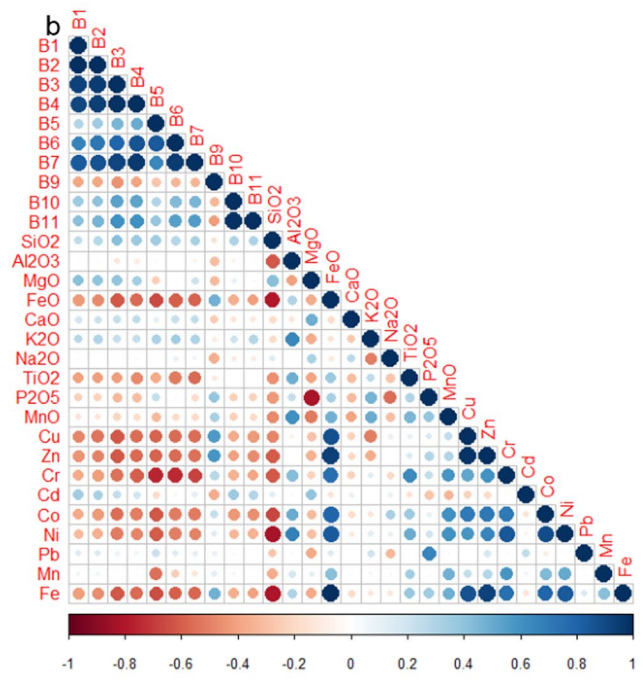
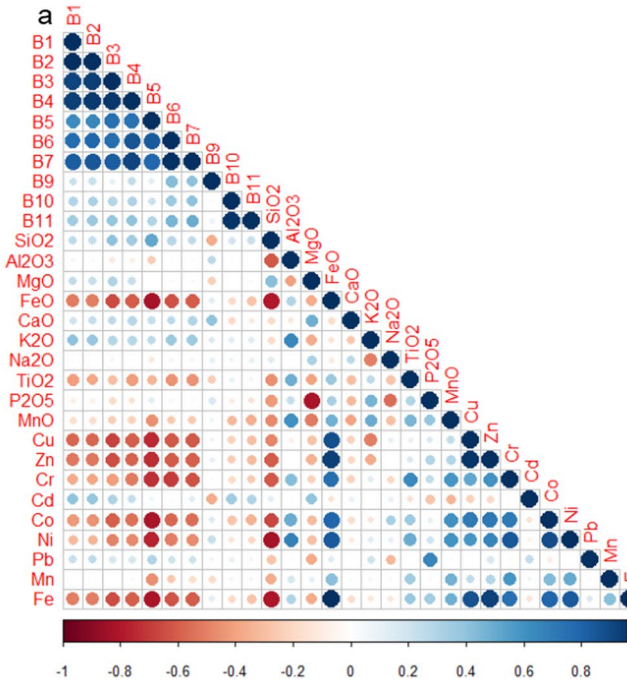
Spectral behavior or reflectance spectroscopy of soil depends on its physical and chemical properties [86]. Visible and near-infrared (VNIR) spectroscopy is a feasible technology for the estimation of heavy metals in soil [87, 88] and potential methodology to be applied in field conditions [89]. Strong correlation between soil spectral reflectance and heavy metal concentration [90] forms a foundation for estimation of heavy metals using imagery.

Vegetation gives high reflectance in the Near Infrared (NIR) region and it is used for the detection of vegetation. Metals (Cu, Zn, Cr, Co and Ni) and FeO show a significant negative correlation with bands 5 (NIR), 6 (SWIR 1) and 9 (cirrus) of the Landsat 8 satellite image of March, 2015 (pre monsoon) while the correlation is not significant in the month of September, 2015 (post monsoon), except for Cr (Fig. 7a). It suggests that in the semi-arid region the metal concentration in soil shows a significant correlation in the dry season. While in the post-monsoon season due to increase in vegetation cover the correlation doesn't show a significant correlation. Similarly, in ground water the concentration of Cu, Co, Ni and Mn shows strong negative correlation with the band 5 (NIR) during pre-monsoon compared to post-monsoon (Fig. 7b). Hence, Cu, Co and Ni show good correlation with band 5 (NIR) in both soil and groundwater during March.

In soil, metals are present in trace quantity, i.e., in ppm and variation in spectral reflectance due to metals seems quite impossible with low-resolution data of landsat 8. Metal concentration in soil is evaluated with NIR and Mid-NIR reflectance spectroscopy [91]. Additionally, spectral reflectance of NIR (reflectance spectroscopy) depends upon soil properties [92] and chemical composition such as organic carbon, inorganic carbon and total nitrogen [93]. Organic matter has high metal sequestration capacity [94] so soil having high organic matter content would also have high metal content. Thus, spectral reflectance is attributed to organic carbon including the metal concentration of soil. But it would be difficult to apply this concept on sites having low content of organic matter like in arid regions or mining areas.

The variation of significant spectral responses with different bands at different concentration of Cu, Ni, Co and Mn is shown in Fig. 8. The spectral reflectance decreases with increase in the concentration of metals such as Cu, Ni, Co and Mn in soil. Choe et al. [95] also reported similar results that a significant correlation between metal concentrations measured at ground level with hyperspectral satellite data and suggests use of hyperspectral data in mapping metal pollution. Hence, high contamination of

a



b

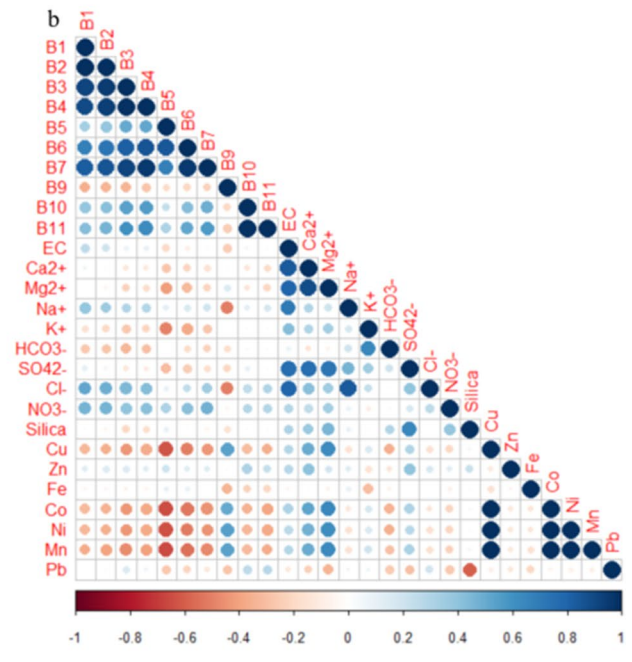
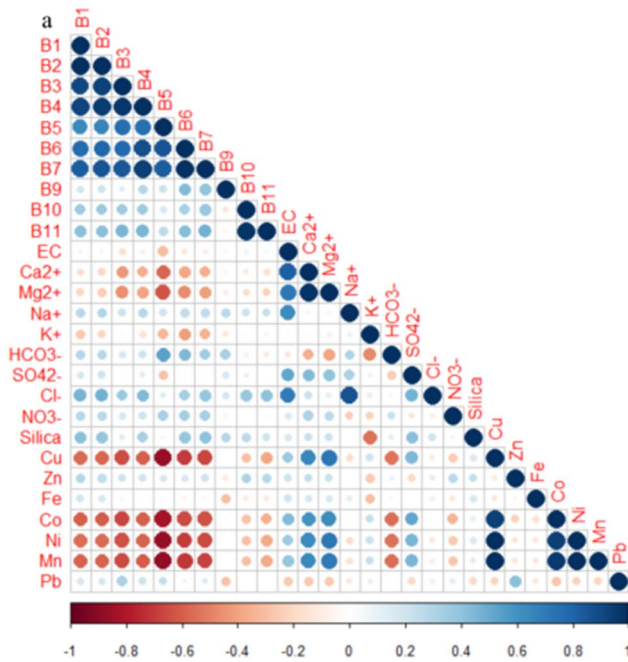


Fig. 7 **a** Correlation of bands with chemical composition of soil **(a)** March **(b)** September **b** Correlation of bands with chemical composition of groundwater **(a)** March **(b)** September

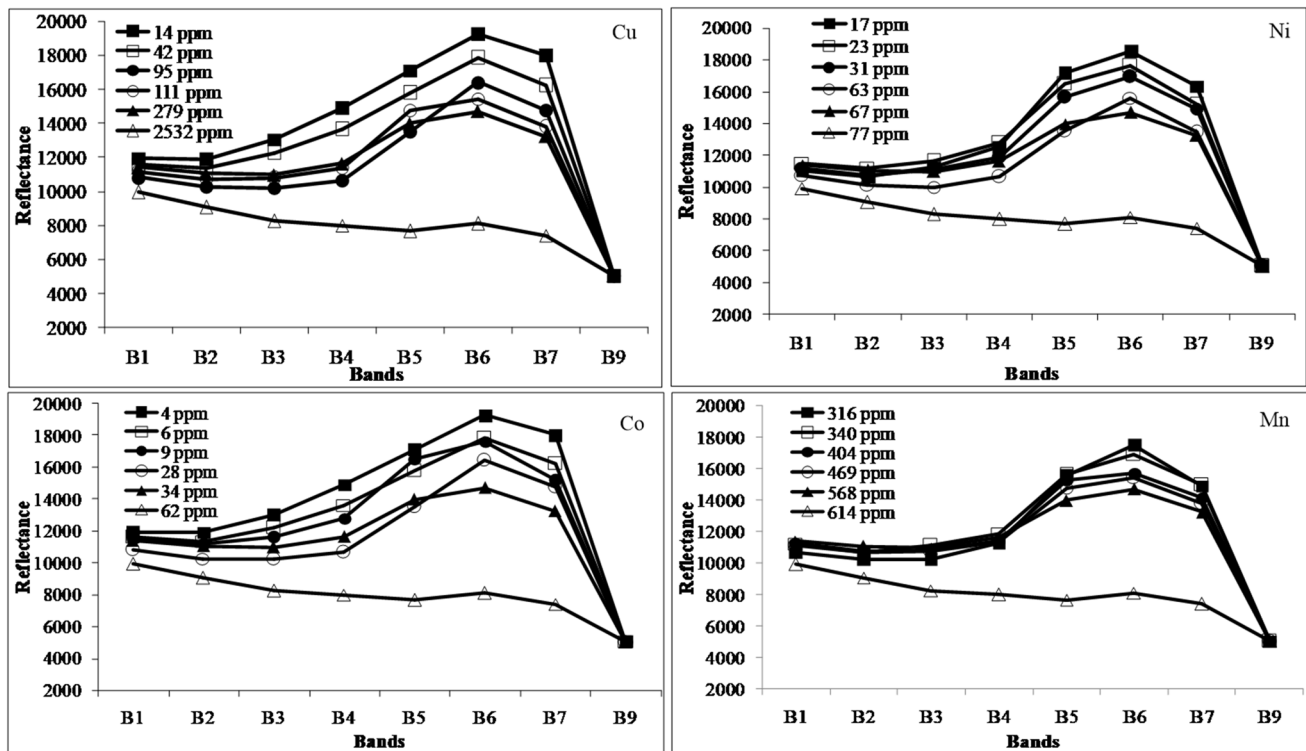


Fig. 8 Spectral reflectance of concentration of Cu, Ni, Co and Mn in soil

metals in soils is possible to be identified using remote sensing data. These results demand further detailed study covering larger area using multi-seasonal satellite data. The assessment of metals in soil and groundwater is time-consuming and needs extensive laboratory work so the correlation studies between spectral responses and metal concentration would facilitate quick assessment of their spatial distribution.

9 Future perspective of research

The spectral resolution of Landsat and ASTER is very low compared to hyperspectral imagery. The present study further demands the application of high-resolution data, i.e., hyperspectral imagery in LULC and estimation of heavy metals. Hyperspectral sensor collects data in hundreds of narrow and adjacent spectral bands depending upon the surface materials such as vegetation and ore deposits. The numerous narrow bands of hyperspectral sensors provide a continuous spectral signature for wide range of electromagnetic spectrum and are more sensitive to slight variations in reflected and emitted energy from the different objects. Main advantages of hyperspectral sensing that it obtains spatial information in two dimensions and spectral information through a number of wavelengths.

Estimated heavy metal concentration and their spectral signature could be integrated for the development of estimation method for heavy metal quantification in soil. Studies have been carried out to develop an estimation model for the estimation of heavy metals or trace elements in soil using spectrometer and spectral reflectance [84, 96–99]. But the feasibility and applicability of estimation models are debatable. More research is needed to explore the feasibility of application of spectral reflectance in estimation of heavy metals at broader scale using satellite imagery for the mining landscape. High concentration of heavy metals in overburden rocks may produce pure peaks of spectral signatures. It may enhance the heavy metal detection accuracy and could be used for referencing. The further research is needed in this aspect as it would further reduce the cost and fast method for the estimation of heavy metals. The present study is in preliminary in nature and needs further research for its application for the fast and easy estimation of heavy metals in the contaminated soil.

10 Conclusions

The increase in metal concentration in soil and groundwater neighboring the mines affects the LULC. Hence, change in LULC in relation with the pollution indices

along with change in pixel values with elemental concentration present in soil and groundwater are studied. A positive rate of change is found in mines, settlement and open area suggesting their spatial increment. The vegetation and water bodies show negative rate of change or their area decreases. The water bodies present till 2012 were vanished in 2017. The declining trend in water resources and vegetation is a cause of concern from the ecological point of view and needs attention of locals and concerned authorities. The fragmentation of landscape pattern due to loss of forest and water bodies results in change in LULC and which is further accelerated due to contamination of soil and water. The loss of agriculture and vegetation near the mines indicates the high impact of pollution on landscape as significant change is observed neighboring the mines and windward direction. It further demands a detailed study for long duration, i.e., for some decades to understand the role of geochemical variation in soil LULC change.

The negative significant correlation between band 5 of Landsat 8 and metal (Cu, Zn, Cr, Co and Ni) concentration of soil and groundwater is found during the pre-monsoon suggesting the possible use of NIR band in the detection of metal concentration in semi-arid region. Decrease in spectral reflectance with wavelength at different concentration of metals demands further detail and systematic study for better results. The main drawback of the study is the non-availability of huge amount of ground level data. However, the study concludes that an integrated approach using field observations and remote sensing inputs can help in better monitoring and assessment of mining landscapes.

Acknowledgements The authors would also like to thank the anonymous reviewers and the editorial board of the journal for constructive comments, suggestions and recommendations on the earlier version of manuscript. AP acknowledges the Council of Scientific and Educational Research (CSIR), Government of India, for providing the necessary funds.

Author contributions AP and PKJ have conceptualized the work. AP carried out data collection and analysis. PKJ and NSS interpreted the results and guided AP to prepared manuscript. All authors equally contributed while reviewing and finalizing the manuscript.

Funding There was no special funding for this research. It has benefited the facilities available with the School of Environmental Sciences, Jawaharlal Nehru University, New Delhi.

Data availability The datasets analyzed during the current study are available from the corresponding author on reasonable request.

Compliance with ethical standards

Conflicts of interest The authors declare that they have no conflict of interest.

Open Access This article is licensed under a Creative Commons Attribution 4.0 International License, which permits use, sharing, adaptation, distribution and reproduction in any medium or format, as long as you give appropriate credit to the original author(s) and the source, provide a link to the Creative Commons licence, and indicate if changes were made. The images or other third party material in this article are included in the article's Creative Commons licence, unless indicated otherwise in a credit line to the material. If material is not included in the article's Creative Commons licence and your intended use is not permitted by statutory regulation or exceeds the permitted use, you will need to obtain permission directly from the copyright holder. To view a copy of this licence, visit <http://creativecommons.org/licenses/by/4.0/>.

References

1. Piervandi Z, Darban AK, Mousavi SM, Mahmoud Abdollahy M, Asadollahfardi G, Funari V, Dinelli E (2019) Minimization of metal sulphides bioleaching from mine wastes into the aquatic environment. *Ecotoxicol Environ Safe* 182:109443
2. Malaviya S, Munsri M, Oinam G, Joshi PK (2010) Landscape approach for quantifying land use land cover change (1972–2006) and habitat diversity in a mining area in Central India (Bokaro, Jharkhand). *Environ Monit Assess* 170:215–229
3. Popelková R, Mulková M (2019) The mining landscape of the Ostrava-Karviná coalfield: processes of landscape change from the 1830s to the beginning of the 21st century. *App Geogr* 90:28–43
4. Charou E, Stefouli M, Dimitrakopoulos D, Vasiliou E, Mavrantza OD (2010) Using remote sensing to assess impact of mining activities on land and water resources. *Mine Water Environ* 29:45–52
5. Grant CD, Ward SC, Morley SC (2007) Return of ecosystem function to restored bauxite mines in western Australia. *Restor Ecol* 15:S94–S103. <https://doi.org/10.1111/j.1526-100X.2007.00297.x>
6. Rudke AP, de Souza VAS, dos Santos AM, Xavier ACF, Filho OCR, Martins JA (2020) Impact of mining activities on areas of environmental protection in the southwest of the Amazon: a GIS- and remote sensing-based assessment. *J Environ Manag* 263:110392
7. Sontter LJ, Moran CJ, Barrett DJ, Soares-Filho BS (2014) Processes of land use change in mining regions. *J Clean Prod* 84:494–501
8. Lechner AM, Baumgartl T, Matthew P, Glenn V (2014) The impact of underground longwall mining on prime agricultural land: a review and research agenda. *Land Degrad Dev* 27:1650–1663
9. Mi J, Yang Y, Hou H, Zhang S, Raval S, Chen Z, Hua Y (2020) The long-term effects of underground mining on the growth of tree, shrub and herb communities in arid and semi-arid areas in China. *Land Degrad Dev*. <https://doi.org/10.1002/ldr.3751>
10. Xiao W, Fu Y, Wang T, Lv X (2018) Effects of land use transitions due to underground coal mining on ecosystem services in high groundwater table areas: a case study in the Yanzhou coalfield. *Land Use Policy* 71:213–221
11. Zhao H, Xia B, Fan C, Zhao P, Shen S (2012) Human health risk from soil heavy metal contamination under different land uses near Dabaoshan Mine, Southern China. *Sci Total Environ* 417–418:45–54
12. Yang X, Lei S, Zhao Y, Cheng W (2020) Use of hyperspectral imagery to detect affected vegetation and heavy metal polluted areas: Shengli mining area, China. *Gecarto Int*. <https://doi.org/10.1080/10106049.2020.1844308>

13. Wu Z, Lei S, Lu Q, Bian Z, Ge S (2020) Spatial distribution of the impact of surface mining on the landscape ecological health of semi-arid grasslands. *Ecol Indic* 111:105996
14. Demirel N, Düzgün Ş, Emil MK (2011) Landuse change detection in a surface coal mine area using multi-temporal high-resolution satellite images. *Int J Min Reclamat Environ* 25(4):342–349
15. Zhu D, Chen T, Zhen N, Niu R (2020) Monitoring the effects of open-pit mining on the eco-environment using a moving window-based remote sensing ecological index. *Environ Sci Pollut Res* 27:15716–15728
16. Awotwi A, Anornu GK, Quaye-Ballard JA, Annor T (2018) Monitoring land-use/land-cover changes due to extensive gold mining, urban expansion and agriculture in the pra river basin of Ghana, 1986–2025. *Land Degrad Dev* 29(10):3331–3343
17. Lei K, Pan H, Lin C (2016) A landscape approach towards ecological restoration and sustainable development of mining areas. *Ecol Eng* 90:320–325
18. Zhang M, Wang J, Li S (2019) Tempo-spatial changes and main anthropogenic influence factors of vegetation fractional coverage in a large-scale opencast coal mine area from 1992 to 2015. *J Clean Prod* 232:940–952
19. Orimoloye IR, Ololade OO (2020) Spatial evaluation of land-use dynamics in gold mining area using remote sensing and GIS technology. *Int J Environ Sci Technol* 17:4465–4480
20. Werner TT, Mudd GM, Schipper AM, Huijbregts MAJ, Taneja L, Northey SA (2020) Global-scale remote sensing of mine areas and analysis of factors explaining their extent. *Glob Environ Change* 60:102007
21. Hendrychová M, Kabrna M (2016) An analysis of 200-year-long changes in a landscape affected by large-scale surface coal mining: History, present and future. *Appl Geogr* 74:151–159
22. Xiao H, Ji W (2007) Relating landscape characteristics to non-point source pollution in mine waste-located watersheds using geospatial techniques. *J Environ Manag* 82:111–119
23. Carrara E, Arroyo-Rodríguez V, Vega-Rivera JH, Schondube JE, de Freitas SM, Fahrig L (2015) Impact of landscape composition and configuration on forest specialist and generalist bird species in the fragmented Lacandona rainforest, Mexico. *Biol Cons* 184:117–126
24. Laurance WF, Sayer J, Cassman KG (2014) Agricultural expansion and its impacts on tropical nature. *Trends Ecol Evol* 29:107–116
25. Turner MG, Ruscher CL (1988) Changes in landscape patterns in Georgia, USA. *Landsc Ecol* 1(4):241–251
26. Miller JR, Schulz TT, Hobbs NT, Wilson KR, Schrupp DL, Baker WL (1995) Changes in the landscape structure of a southeastern Wyoming riparian zone following shifts in stream dynamics. *Biol Conserv* 72(3):371–379
27. Kusimi JM (2008) Assessing land use and land cover change in the Wassa West District of Ghana using remote sensing. *GeoJournal* 71:249–259
28. Tongway DJ, Ludwig JA (1994) Small-scale resource heterogeneity in semi-arid landscapes. *Pac Conserv Biol* 1(3):201–208
29. Tongway DJ, Valentin C, Seghieri J (2001) Banded vegetation patterning in arid and semiarid environments: ecological processes and consequences for management. Springer, New York, pp 132–145
30. Roychowdhury MK, Dasgupta SP (1964) On the geology and mineralization in the Khetri copper belt, Jhnujhuu and Sikar districts, Rajasthan. *Geol Sur India* 31:188–198
31. GSI MIS. PUB (2011) Geology and mineral resources of Rajasthan: Geological Survey of India: Miscellaneous Publication No. 30 Part 12, 3rd revised edition
32. Verma D, Jadhav GN, Biswal TK, Jena SK, Sharma N (2012) Characterization of hydrocarbon-bearing fluid inclusion in sandstones of Jaisalmer basin, Rajasthan: a preliminary approach. *J Geol Soc India* 80(4):515–524
33. Punia A, Siddaiah NS, Singh SK (2017) Source and assessment of heavy metal pollution at Khetri copper mine tailings and surrounding soil, Rajasthan, India. *Bull Environ Contam Toxicol* 99:633–641
34. Qin C, Luo C, Chen Y, Shen Z (2012) Spatial-based assessment of metal contamination in agricultural soils near an abandoned copper mine of eastern China. *Bull Environ Contam Toxicol* 89:113–118
35. Gong X, Chen Z, Luo Z (2014) Spatial distribution, temporal variation, and sources of heavy metal pollution in groundwater of a century-old nonferrous metal mining and smelting area in China. *Environ Monit Assess* 186:9101–9116
36. Gallwey J, Robiati C, Coggan J, Vogt D, Eyre M (2020) A sentinel-2 based multispectral convolutional neural network for detecting artisanal small-scale mining in Ghana: applying deep learning to shallow mining. *Remote Sens Environ* 248:111970. <https://doi.org/10.1016/j.rse.2020.111970>
37. Modiegi M, Rampedti IT, Tesfamichael SG (2020) Comparison of multi-source satellite data for quantifying water quality parameters in a mining environment. *J Hydrol* 591:125322
38. Sagan V, Peterson KT, Maimaitijiang M, Sidike P, Sloan J, Greeling BA, Maalouf S, Adams C (2020) Monitoring inland water quality using remote sensing: potential and limitations of spectral indices, bio-optical simulations, machine learning, and cloud computing. *Earth-Sci Rev* 205:103187
39. Abdelmalik KW (2018) Role of statistical remote sensing for Inland water quality parameters prediction. *Egypt J Remote Sens Space Sci* 21:193–200
40. Wu Y, Chen J, Wu X, Tian Q, Ji J, Qin Z (2005) Possibilities of reflectance spectroscopy for the assessment of contaminant elements in suburban soils. *Appl Geochem* 20(6):1051–1059
41. Kooistra L, Wehrens R, Leuven RSEW, Buydens LMC (2001) Possibilities of visible-near infrared spectroscopy for the assessment of soil contamination in river floodplains. *Anal Chim Acta* 446(1):97–105
42. Sun W, Zhang X (2017) Estimating soil zinc concentrations using reflectance spectroscopy. *Int J Appl Earth Obs* 58:126–133
43. Nadari A, Delavar MA, Kaboudin B, Askari MS (2017) Assessment of spatial distribution of soil heavy metals using ANN-GA, MSLR and satellite imagery. *Environ Monit Assess* 189:214
44. Kemper T, Sommer S (2002) Estimate of heavy metal contamination in soils after mining accident using reflectance spectroscopy. *Environ Sci Technol* 12(36):2742–2747
45. Ren H-Y, Zhuang D, Singh AN, Pan J, Qiu D, Shi R (2009) Estimation of As and Cu contamination in agricultural soils around a mining area by reflectance spectroscopy; a case study. *Pedosphere* 19(6):719–726
46. Soydan H, Düzgün HS, Özdemir OB (2015) Analysis of land use land cover changes for an abandoned mine site. In: 2015 IEEE International Geoscience and Remote Sensing Symposium (IGARSS), Milan. IEEE, pp 3049–3052. <https://doi.org/10.1109/IGARSS.2015.7326459>
47. Fan X, Liu Y (2016) A global study of NDVI difference among moderate-resolution satellite sensors. *ISPRS J Photogramm Remote Sens* 121:177–191
48. Liang SZ, Ma WD, Sui XY, Yao HM, Li HZ, Liu T, Wang M (2017) Extracting the spatiotemporal pattern of cropping systems from NDVI time series using a combination of the spline and HANTS Algorithms: a case study for Shandong Province. *Can J Remote Sens* 43(1):1–15
49. Rahman MTU, Tabassum F, Rasheduzzaman M, Saba H, Sarkar L, Ferdous J, Uddin SZ, Islam Z (2017) Temporal dynamics of land use/land cover change and its prediction using CAANN model

- for southwestern coastal Bangladesh. *Environ Monit Assess* 189:565
50. Hussain S, Mubeen M, Ahmad A, Akram W, Hammad HM, Ali M, Masood N, Amin A, Farid HU, Sultana SR, Fahad S, Wang D, Nasim W (2020) Using GIS tools to detect the land use/land cover changes during forty years in Lodhran District of Pakistan. *Environ Sci Poll Res* 27:39676–39692
 51. Fatemi M, Narangifard M (2019) Monitoring LULC changes and its impact on the LST and NDVI in District 1 of Shiraz City. *Arab J Geosci* 12:127
 52. Sousa da Silva V, Salami G, Oliveira da Silva MI, Silva EA, Monteiro Junior JJ, Alba E (2020) Methodological evaluation of vegetation indexes in land use and land cover (LULC) classification. *Geol Ecol Lands* 4(2):159–169
 53. Yang Y, Erskine PD, Zhang S, Wang Y, Bian Z, Lei S (2018) Effects of underground mining on vegetation and environmental patterns in a semi-arid watershed with implications for resilience management. *Environ Earth Sci* 77:605
 54. Donggan G, Zhongke B, Tieliang S, Hongbo S, Wen Q (2011) Impacts of coal mining on the aboveground vegetation and soil quality: a case study of qinxin coal mine in Shanxi Province, China. *Clean Soil Air Water* 39(3):219–225
 55. McGarigal K, Cushman SA, Ene E (2012) FRAGSTATS v4: spatial pattern analysis program for categorical and continuous maps. Computer software program produced at the University of Massachusetts, Amherst. <http://www.umass.edu/landeco/research/fragstats/fragstats.html>
 56. Jenerette GD, Wu J (2001) Analysis and simulation of land-use change in the central Arizona-Phoenix region, USA. *Landsc Ecol* 16:611–626
 57. Lamine S, Petropoulos GP, Singh SK, Szabó S, Bachari NEI, Srivastava PK, Suman S (2017) Quantifying land use/land cover spatio-temporal landscape pattern dynamics from Hyperion using SVMs classifier and FRAGSTATS®. *Geocarto Int* 6049:1–17
 58. Wu J (2007) *Landscape ecology: pattern, process, scale and hierarchy*, 2nd edn. Higher Education Press, Beijing
 59. Punia A, Siddaiah NS (2017) Assessment of heavy metal contamination in groundwater of Khetri copper mine region, India and health risk assessment. *Asian J Water Environ Pollut* 14(4):9–19
 60. Zhang M, Wang J, Feng Y (2019) Temporal and spatial change of land use in a large-scale opencast coal mine area: a complex network approach. *Land Use Policy* 86:375–386
 61. Ererer A (2011) Remote sensing of vegetation health for reclaimed areas of Seyitömer open cast coal mine. *Int J Coal Geo* 86(1):20–26
 62. Kamga MA, Fils SCN, Ayodele MO, Olatubara CO, Nzali S, Adenikinju A, Khalifa M (2020) Evaluation of land use/land cover changes due to gold mining activities from 1987 to 2017 using landsat imagery, East Cameroon. *GeoJournal* 85:1097–1114
 63. Nielsen HD, Brownlee C, Coelho SM, Brown M (2003) Interpopulation differences in inherited copper tolerance involve photosynthetic adaptation and exclusion mechanisms in *Fucus seratus*. *New Phytol* 160:157–165
 64. Demirevska-Kepova K, Simova-Stoilova L, Stoyanova Z, Holzer R (2004) Biochemical changes in barley plants after excessive supply of copper and manganese. *Environ Exper Bot* 52(3):253–266
 65. Lesschen JP, Cammeraat LH, Kooijman AM, Wesemael BV (2008) Development of spatial heterogeneity in vegetation and soil properties after land abandonment in a semi-arid ecosystem. *J Arid Environ* 72:2082–2092
 66. Gunson AJ, Klein B, Veiga M, Dunbar S (2012) Reducing mine water requirements. *J Clean Prod* 21(1):71–82
 67. Gunson A, Klein B, Veiga M (2010) Estimating global water withdrawals due to copper mining. In: Wiertz J (ed) *International congress on water management in the mining industry*. ECAMIN, Santiago
 68. Garai D, Narayana AC (2018) Land use/land cover changes in the mining area of Godavari coal fields of southern India. *Egypt J Remote Sens Space Sci* 21:375–381
 69. Obodai J, Adjei KA, Odai SN, Lumor M (2019) Land use/land cover dynamics using landsat data in a gold mining basin-the Ankobra, Ghana. *Remote Sens Appl Soc Environ* 13:247–256
 70. Cao Y, Bai Z, Zhou W, Zhang X (2016) Characteristic analysis and pattern evolution on landscape types in typical compound area of mine agriculture urban in Shanxi Province. *China Environ Earth Sci* 75:585
 71. Mirzaei M, Jafari A, Gholamalifard M, Azadi H, Shooshtari SJ, Moghaddam SM, Gebrehiwot K, Witlox F (2020) Mitigating environmental risks: modeling the interaction of water quality parameters and land use cover. *Land Use Policy* 95:103766
 72. Kumar M, Denis DM, Singh SK, Szabó S, Suryavanshi S (2018) Landscape metrics for assessment of land cover change and fragmentation of a heterogeneous watershed. *Rem Sens Appl Soc Environ* 10:224–233
 73. Qian D, Yan C, Xing Z, Xiu L (2017) Monitoring coal mine changes and their impact on landscape patterns in an alpine region: a case study of theMuli coal mine in the Qinghai-Tibet Plateau. *Environ Monit Assess* 189:559
 74. Quanyuan W, Jiewu P, Shanzhong Q, Yiping L, Congcong H, Tingxiang L, Limei H (2009) Impacts of coal mining subsidence on the surface landscape in Longkou city, Shandong Province of China. *Environ Earth Sci* 59:783–791
 75. Zhang M, Wang J, Li S, Feng D, Cao E (2020) Dynamic changes in landscape pattern in a large-scale opencast coal mine area from 1986 to 2015: a complex network approach. *CATENA* 194:104738
 76. Gao JF, Ma KM, Feng ZW, Qi J, Feng Y (2009) Coupling effects of altitude and human disturbance on landscape and plant diversity in the vicinity of mountain villages of Beijing, China. *Acta Ecol Sin* 29:56–61
 77. Dadhich PN, Hanaoka S (2016) Remote sensing application in monitoring impact of mining activities on urban growth. Case of makrana marble mines, India. *J Sett Spat plan* 7(2):179–185
 78. Lamichhane S, Shakya NM (2020) Shallow aquifer groundwater dynamics due to land use/cover change in highly urbanized basin: the case of Kathmandu Valley. *J Hydrol Reg Stud* 30:100707
 79. Clarke KC, Salmanmahiny A, Najafinejad A (2014) Water quality restoration using landscape metrics analysis: a case study in the Golestan Province of Iran. *Environ Resour Res* 2(1):77–94
 80. Liu X, Bai Z, Zhou W, Cao Y, Zhang G (2017) Changes in soil properties in the soil profile after mining and reclamation in an open-cast coal mine on the Loess Plateau, China. *Ecol Eng* 98:228–239
 81. Zu Y, Li Y, Christian S, Laurent L, Liu F (2004) Accumulation of Pb, Cd, Cu and Zn in plants and hyperaccumulator choice in Lanping lead-zinc mine area, China. *Environ Int* 30:567–576
 82. Chatterjee J, Chatterjee C (2000) Phytotoxicity of cobalt, chromium and copper in cauliflower. *Environ Poll* 109(1):69–74
 83. Swayze GA, Smith KS, Clark RN, Sutley SJ, Pearson RM, Vance JS, Hageman PL, Briggs PH, Al M, Singleton MJ, Roth S (2000) Using imaging spectroscopy to map acidic mine waste. *Environ Sci Technol* 34:47–54
 84. Sun W, Skidmore AK, Wang T, Zhang X (2019) Heavy metal pollution at mine sites estimated from reflectance spectroscopy following correction for skewed data. *Environ Poll* 252:1117–1124
 85. Shi T, Chen Y, Liu Y, Wu G (2014) Visible and near-infrared reflectance spectroscopy-An alternative for monitoring soil contamination by heavy metals. *J Hazard Mat* 265:166–176
 86. Stoner ER, Baumgardner MF (1981) Characteristic variations in reflectance of surface soils. *Soil Sci Soc Am J* 45:1161–1165
 87. Liu J, Zhang Y, Wang H, Du Y (2018) Study on the prediction of soil heavy metal elements content based on visible

- near-infrared spectroscopy. *Spectrochim Acta A Mol Biomol Spectrosc* 199:43–49
88. Cheng H, Shen R, Chen Y, Wan Q, Shi T, Wang J, Wang Y, Hong Y, Li X (2019) Estimating heavy metal concentrations in suburban soils with reflectance spectroscopy. *Geoderma* 336:59–67
 89. Zhang X, Sun W, Cena Y, Zhang L, Wang N (2019) Predicting cadmium concentration in soils using laboratory and field reflectance spectroscopy. *Sci Total Environ* 650:321–334
 90. Choe E, Kim KW, Bang S, Yon IH, Lee KY (2009) Quantitative analysis and mapping of heavy metals in an abandoned Au-Ag mine area using NIR spectroscopy. *Environ Geol* 58:477–482
 91. Siebielec G, McCarty GW, Stuczynski TI, Reeves JB (2004) Near- and mid-infrared diffuse reflectance spectroscopy for measuring soil metal content. *J Environ Qual* 33(6):2056–2069
 92. Rossel RAV, Walvoort DJJ, Mcbratney AB, Janik LJ, Skjrmstad JO (2006) Visible, near infrared, mid infrared or combined diffuse reflectance spectroscopy for simultaneous assessment of various soil properties. *Geoderma* 131(1–2):59–75
 93. Cheng-Wen C, David L (2002) Near-infrared reflectance spectroscopic analysis of soil C and N. *Soil Sci* 167(2):110–116
 94. Uchimiya M, Lima IM, Klasson KT, Wartelle LM (2010) Contaminant immobilization and nutrient release by biochar soil amendment: roles of natural organic matter. *Chemosphere* 80(8):935–940
 95. Choe E, Meer FVD, Ruitenbeek FV, Werff HVD, Smeth BD, Kim KW (2008) Mapping of heavy metal pollution in stream sediments using combined geochemistry, field spectroscopy, and hyperspectral remote sensing: A case study of the Rodalquilar mining area, SE Spain. *Remote Sens Environ* 112:3222–3233
 96. Khosravi V, Ardejani FD, Yousefi S (2017) Spectroscopic-based assessment of the content and geochemical behaviour of arsenic in a highly heterogeneous sulphide-rich mine waste dump. *Environ Earth Sci* 76(13):459
 97. Tan K, Wang H, Zhang Q, Jia X (2018) An improved estimation model for soil heavy metal(loid) concentration retrieval in mining areas using reflectance spectroscopy. *J Soils Sediments* 18:2008–2022
 98. Purwadi I, van der Werff H, Lievens C (2019) Reflectance spectroscopy and geochemical analysis of rare earth element bearing tailings: a case study of two abandoned tin mine sites in Bangka Island, Indonesia. *Int J Appl Earth Obs Geoinform* 74:239–247
 99. Raval S, Shamsoddini A (2014) A monitoring framework for land use around kaolin mining areas through Landsat TM images. *Earth Sci Inform* 7:153–163

Publisher's Note Springer Nature remains neutral with regard to jurisdictional claims in published maps and institutional affiliations.